

# DS-CDMA Chip Waveforms with Maximally Concentrated Spectra

Ritesh Sood  
Department of Elect. & Comp. Eng.  
University of California, Davis  
Email: rsood@ucdavis.edu

Hong Xiao  
Department of Mathematics  
University of California, Davis  
Email: hxiao@ucdavis.edu

**Abstract**—We propose chip waveforms for essentially full-response signaling in DS-CDMA systems that employ offset quadrature modulation formats. The waveforms are optimal in the sense that for a given out of band power leakage, the transmit signal occupies the minimum inband power bandwidth. At the same time, certain smoothness conditions on the phase and envelope of the transmit signal in the time domain are satisfied. The performance of the respective modulation schemes is compared with that of conventional techniques including MSK and time-domain raised-cosine pulses. Numerical results indicate a significant gain in system capacity compared to conventional pulses, and near optimality with respect to interference rejection.

## I. INTRODUCTION

A method for the synthesis of chip waveforms for direct-sequence code-division multiple-access (DS-CDMA) communications systems is proposed. The DS-CDMA systems that we consider employ offset linear quadrature modulation, random signature sequences, and single-user correlation receivers. Offset quadrature phase-shift keying (OQPSK) with rectangular chip waveform, and minimum-shift keying (MSK) with half-sine chip waveform are common examples of the class of systems mentioned above.

Various performance parameters of DS-CDMA systems benefit from a carefully designed signaling pulse. These benefits include bandwidth efficiency, resilience to interference, and ease of hardware implementation. While the rectangular and raised cosine pulses have been predominant in practice, it should be kept in mind that these pulses are suboptimal in channels that suffer from multiple access interference (MAI) in addition to additive Gaussian noise. In recent years, research has been directed towards the synthesis of signaling pulses that are more suited to modern communication environments characterized by multiple simultaneous users, high data-rates, and various forms of diversity [1]–[3].

It is well known that pulse shaping in linear modulation schemes improves the spectral efficiency of the communication system [4]. This improvement is particularly important in DS-CDMA systems, since it allows the use of longer spreading codes for the same bandwidth requirement. As a result, the overall system capacity is improved, since it is possible to accommodate more users at the same bit-error

rate, or reduce the bit-errors per user for the same number of users. Furthermore, in DS-CDMA systems employing single-user correlation receivers, the pulse signal affects the received signal to interference and noise ratio (SINR) through its auto-correlation function. Thus the bit error rate (BER) performance of a DS-CDMA system may be improved by shaping the chip waveform in an optimal manner, which results in further gains in system capacity.

### A. Previous work and our contributions

Various optimality criteria have been previously used for the design of DS-CDMA chip waveforms. Among these are minimum MAI power, minimum squared correlation of the chip waveform [5], and minimum rms bandwidth for signal sets with pairwise signal correlation constraints. The performance of commonly known pulse shapes—those based on the Hanning window for instance—has been reported in several papers (see [2] and references therein).

A shortcoming of methods that rely on optimizing any of the cost functions mentioned above is that the resulting optimization problem is often non-convex. For example, expressions for the squared correlation of the shaping pulse, and the variance of the MAI signal components are usually obtained as polynomials in the optimization parameters. Since the degree of these polynomials is generally greater than two, resulting objective functions are non-convex. Furthermore, a constant energy constraint imposed on the pulse waveform results in a non-convex feasible set. Hence, numerical optimization techniques applied to these problems often return solutions that are not globally optimal.

Keeping in mind the pitfalls of formulating and numerically solving a non-convex optimization problem, we adopt an alternate approach in this paper. In a previous work [4] the authors have presented a numerically efficient global optimization procedure for the design of root-Nyquist pulses with maximum spectral energy concentration. This paper extends the above method to the design of DS-CDMA chip waveforms that satisfy certain smoothness conditions on the phase and envelope of the transmit signal, and are optimal in terms of bandwidth occupancy of the power spectrum. Numerical results show significant capacity increase compared to conventional signaling schemes using MSK and time-domain raised-cosine pulses. While not explicitly designed to minimize

This work was supported in part by the NSF under grants DMS-0513069 and DMS-0135345.

the MAI power, the pulses are nearly optimal in terms of interference rejection.

## II. SYSTEM MODEL

We consider a single-cell DS-CDMA reverse link (mobile to base) channel with  $K$  active users transmitting in the offset-QPSK (OQPSK) format [6]. The in-phase and quadrature components of the baseband information signal for the  $k^{\text{th}}$  user are expressed as

$$\begin{aligned} b_k^I(t) &= \sum_{l=-\infty}^{\infty} b_{k,l}^I \text{rect}_T(t - lT) \\ b_k^Q(t) &= \sum_{l=-\infty}^{\infty} b_{k,l}^Q \text{rect}_T(t - lT) \end{aligned} \quad (1)$$

respectively. In (1), superscripts  $I$  and  $Q$  denote, respectively, the in-phase and quadrature components,  $\text{rect}_T(t)$  denotes the unit pulse on the interval  $[0, T]$ , and  $b_{k,l}^I, b_{k,l}^Q \in \{-1, +1\}$  are the information bits modeled as binary random variables with equal probability. Spectrum spreading is achieved by multiplying the information signal with the spreading signals

$$\begin{aligned} a_k^I(t) &= \sum_{m=-\infty}^{\infty} a_{k,m}^I p'(t - mT_c), \\ a_k^Q(t) &= \sum_{m=-\infty}^{\infty} a_{k,m}^Q p'(t - mT_c), \end{aligned}$$

with  $(a_k^I)$  and  $(a_k^Q)$  being the pseudo-random, aperiodic signature sequences of the  $k^{\text{th}}$  user, and  $a_{k,m}^I, a_{k,m}^Q \in \{-1, +1\}$  the independent  $m^{\text{th}}$  chip symbols at chip rate  $1/T_c$  with equal probabilities of being 1 or  $-1$ . It is assumed that the spreading factor  $N = T/T_c$  is an integer. We represent the real valued transmit chip waveform as  $p'(t)$ , which has duration  $T_p \geq T_c$  and is symmetric about  $t = T_c/2$ .

We denote by  $\kappa = \frac{T_p}{2T_c}$  the normalized one sided excess time duration of  $p(t)$ . The case  $\kappa = 0.5$  corresponds to full response signaling, and matched filtering at the receiver introduces no inter symbol interference (ISI) at the chip level. It is convenient to define the shifted pulse  $p(t) = p'(t + T_c/2)$ , where  $t \in [-T_p/2, T_p/2]$ . Thus,  $p(t)$  is centered, and is symmetric about  $t = 0$ . It follows that the corresponding matched pulse,  $g(t) = p(t) \star p(-t)$ , is symmetric and time-limited to the interval  $[-T_p, T_p]$ . We normalize  $p(t)$  so that its net energy satisfies  $g(0) = \int_{-T_p/2}^{T_p/2} |p(t)|^2 dt = T_c$ .

The two quadrature carriers are modulated by the baseband signals, and a time offset of  $T_c/2$  is introduced in the cosine branch to yield the passband signals as

$$s_k^I(t) = a_k^I(t - T_c/2) b_k^I(t - T_c/2) \cos(\omega_c t + \theta_k), \quad (1)$$

$$s_k^Q(t) = a_k^Q(t) b_k^Q(t) \sin(\omega_c t + \theta_k), \quad (2)$$

where  $\omega_c$  denotes the carrier angular frequency, and  $\theta_k$  the phase offset of the  $k^{\text{th}}$  user. The transmitted signal is thus

$$s_k(t) = s_k^I(t) + s_k^Q(t). \quad (3)$$

We consider asynchronous receptions at the receiver and denote by  $\tau_k$  the time delay of the  $k^{\text{th}}$  user's signal. The net

received signal  $r(t)$  is then

$$r(t) = \sum_{k=1}^K s_k^I(t - \tau_k) + s_k^Q(t - \tau_k) + w(t),$$

where  $w(t)$  is additive white Gaussian noise process with power spectral density  $N_0/2$ . The delays  $\tau_k$  are interpreted modulo- $T_c$  and are modeled as random variables distributed uniformly in the intervals  $[0, T_c]$ .

In this paper, we consider a single user, symbol-by-symbol detector that employs matched filtering. The user with index  $k = 1$  is designated the user of interest, and the receiver is assumed to be synchronized to the signal of this user. Thus,  $\tau_1 = 0$ , and the delays of the remaining users are relative to that of the first user. Due to the symmetry in the the in-phase and quadrature components of the transmitted signal (1) and (2), it is sufficient to consider either one, and without loss of generality, we consider the quadrature component in the rest of the paper. The soft estimate of the transmitted symbol is obtained by matched filtering the received signal  $r(t)$  as

$$Z_1^Q(t) = \int_{t-T-t'}^{t+t'} r(\tau) a_1^Q(\tau) \sin(\omega_c \tau) d\tau, \quad (4)$$

where  $t' = (\kappa - 1)T_c/2$ . Sampling  $Z_1^Q(t)$  at  $t = iT$  followed by threshold detection provides an estimate  $\hat{b}_{1,i-1}^Q$  of the  $(i-1)^{\text{th}}$  transmitted bit.

## III. CHIP WAVEFORMS AND SYSTEM CAPACITY

### A. Spectral efficiency

The bandwidth requirement of a linear modulation scheme is characterized by the power spectral density (PSD) of the baseband transmit signal. A commonly used measure for bandwidth is the *in-band power bandwidth*, which is defined as the frequency interval  $[-W, W]$  that contains a prescribed fraction  $1 - \eta$  of the signal power. Since the data and chip symbols in our model are i.i.d. binary random variables, the PSD is proportional to the squared magnitude of the Fourier transform  $P(f)$  of the chip waveform. As a result, the in-band power bandwidth is defined by the relation

$$\frac{\int_{-W}^W |P(f)|^2 df}{\int_{-\infty}^{\infty} |P(f)|^2 df} = 1 - \eta.$$

The values  $\eta = 10^{-4}$ , or  $\eta = 10^{-5}$  are commonly used in practice.

Since  $p(t)$  is time-limited, the in-band energy ratio  $1 - \eta$  for given a  $T_p$  and  $W$  pair cannot be made arbitrarily close to 1. Indeed, the Uncertainty Principle [7] lays down a tight upper-bound on  $1 - \eta$ , which increases as the time-bandwidth product  $WT_p$  increases. Thus, for a given  $\eta$ , the in-band power bandwidth  $W$  can be reduced by employing partial-response pulses (*i.e.*  $T_p > T_c$ , or  $\kappa > 0.5$ ). On the other hand, inter-symbol interference resulting from time offset in the receiver's clock is minimum when full-response chip waveforms are employed. As a trade-off between these two

conflicting requirements, we consider pulses that have  $\kappa$  in the range of 0.5–1.0.

In this paper, we impose a continuous phase requirement on  $p(t)$  (see Section III-C), which leads to small amplitudes for the auto-correlation function  $g(t)$  for  $|t| \geq T_c$ . Thus, while spectral efficiency is gained due to a larger time-bandwidth product  $WT_p$ , the desirable ISI properties of full response pulses are retained. We call a pulse  $p(t)$  with  $\kappa$  in the above range an *essentially* full-response pulse.

### B. SINR performance

It is well known that in a pure AWGN channel with matched filtering, the transmitted pulse affects the received SNR only through its energy, *i.e.* signaling pulses that have different shapes but the same energy result in the same SNR. In a DS-CDMA system however, as a result of MAI, the shape of the chip waveform affects the received SINR through its auto-correlation function.

Denoting by  $M_c$  the normalized mean-squared chip correlation:

$$M_c = \frac{1}{T_c^3} \int_0^{T_c} g^2(\tau) d\tau + \frac{1}{T_c^3} \int_{T_c}^{T_p} g^2(\tau) d\tau, \quad (5)$$

the following expression for the received SINR in OQPSK modulation with random spreading is obtained [5], [6]:

$$\text{SINR} = \frac{[\mathbb{E}[Z_1^Q(T)]]^2}{\text{var}[Z_1^Q(T)]} = \frac{2E_b}{N_0 + 4(K-1)E_b \frac{M_c}{N}}. \quad (6)$$

It can be seen that the shaping pulse, through its auto-correlation function, has a direct bearing on the received SINR, and hence on the system error performance. It can also be seen that in the absence of additive noise ( $N_0 = 0$ ), the SINR is proportional to the ratio  $N/M_c$ .

Consider two systems  $i = 1, 2$ , employing different chip waveforms at chip-rates  $1/T_c^{(i)}$ , spreading factors  $N^{(i)}$ , mean squared correlations  $M_c^{(i)}$ , and for a given  $\eta$ , in-band power bandwidths  $W^{(i)}$ . The SINR gain of system 1 over system 2 is thus quantified by the ratio

$$\frac{N^{(1)}M_c^{(2)}}{N^{(2)}M_c^{(1)}}. \quad (7)$$

Imposing equal bit-rate  $1/T$  and in-band power bandwidth  $W^{(1)} = W^{(2)} = W$  on the two systems, we have that

$$\frac{N^{(1)}}{N^{(2)}} = \frac{TT_c^{(2)}}{TT_c^{(1)}} = \frac{WT_c^{(2)}}{WT_c^{(1)}}. \quad (8)$$

The combination of (8) and (7) implies that the SINR gain is

$$\frac{WT_c^{(2)} \times M_c^{(2)}}{WT_c^{(1)} \times M_c^{(1)}}.$$

Accordingly, we adopt  $WT_c \times M_c$  as a measure of the effect of chip waveform shaping on system capacities.

### C. Phase continuity and envelope uniformity

It is desirable that the transmit signal has a continuous phase, since such a signal is less prone to transient and high-order harmonic generation by hardware circuitry. It can be shown [5] that continuous phase transitions are ensured if  $p(t)$  is continuous and vanishes at its end points. Since  $p(t)$  is symmetric, the required constraint—in addition to continuity in the open interval  $(-T_p/2, T_p/2)$ —is that

$$p(T_p/2) = 0. \quad (9)$$

The envelope of the transmitted signal is obtained from (1) and (2) as

$$e(t) \approx \begin{cases} \sqrt{p^2(t) + p^2(t + \frac{T_c}{2})} & -\frac{T_p}{2} \leq t < 0, \\ \sqrt{p^2(t) + p^2(t - \frac{T_c}{2})} & 0 \leq t < \frac{T_p}{2}. \end{cases} \quad (10)$$

The variation of  $e(t)$  is measured by the amplitude modulation (AM) index defined as

$$\text{AM index} = \frac{\max e(t) - \min e(t)}{\max e(t) + \min e(t)},$$

which should be kept as low as possible to prevent spectral regrowth in the RF amplification stage. It can be shown [5] that the condition

$$p(0) = \sqrt{2}p(T_c/4) \quad (11)$$

leads to a nearly constant envelope. We adopt the above criterion for envelope uniformity, since it is linear, and is easily incorporated in the optimization problem formulated later in the paper. Following [5], pulses that satisfy (11) are said to have a *quasi-uniform envelope* (QUE).

## IV. PROPOSED METHOD

In order to formulate the problem in a finite dimensional setting, we project the pulse function onto a finite subset of the prolate spheroidal wave functions (PSWFs) [7] as

$$p(t) = \sum_{m=0}^{M-1} x_m \psi_{2m}(t), \quad P(f) = \sum_{m=0}^{M-1} x_m \Psi_{2m}(t), \quad (12)$$

where  $\psi_m$  is the  $m^{\text{th}}$  order PSWF corresponding to the parameter  $c = \pi WT_p$ , and  $\Psi_m$  is its Fourier transform. Denoting by  $\mathbf{x} = [x_0, \dots, x_{M-1}]^T$  the vector of coefficients in (12), the in-band energy of  $P(f)$  is written as

$$\int_{-W}^W |P(f)|^2 df = \mathbf{x}^T H_0 \mathbf{x}, \quad (13)$$

where  $[H_0]_{m,m} = \int_{-W}^W |\Psi_m(f)|^2 df$ . Since  $g(t)$  is time-limited, each chip-symbol experiences ISI from  $I = \lfloor 2\kappa \rfloor$  symbols on either side. The interference terms  $g(iT_c)$  are obtained as

$$g(iT_c) = \mathbf{x}^T H_i \mathbf{x} \quad \text{for } i = \pm 1, \dots, \pm I, \quad (14)$$

where  $[H_i]_{m,n} = \int_{-T_p/2}^{T_p/2} \psi_m(t) \psi_n(t - iT_c) dt$ .

In order to incorporate the continuous phase and uniform envelope conditions, we define the vectors  $\mathbf{c}_1, \mathbf{c}_2 \in \mathbb{R}^M$  as

$$[\mathbf{c}_1]_m = \psi_m(T_p/2), \quad [\mathbf{c}_2]_m = \psi_m(0) - \sqrt{2}\psi_m(T_p/4),$$

and denote by  $\mathcal{C}$  the subspace spanned by  $\{\mathbf{c}_1, \mathbf{c}_2\}$ . Collecting these vectors on the columns of the  $M \times 2$  matrix  $C = [\mathbf{c}_1 \ \mathbf{c}_2]$ , the constraints (9) and (11) are then written as

$$C^T \mathbf{x} = \mathbf{0}. \quad (15)$$

Let the orthogonal complement of  $\mathcal{C}$  be denoted by  $\mathcal{C}^\perp$ , and let the matrix  $C^\perp$  consist of an orthonormal set of basis vectors for  $\mathcal{C}^\perp$ . Then, all vectors  $\mathbf{x} \in \mathcal{C}^\perp$ , *i.e.*, vectors of the form  $\mathbf{x} = C^\perp \mathbf{y}$  satisfy (15), where  $\mathbf{y}$  is arbitrary. By restricting  $\mathbf{x}$  to  $\mathcal{C}^\perp$ , and defining the matrices

$$\tilde{H}_0 = (C^\perp)^T H_0 C^\perp, \quad \tilde{H}_i = (C^\perp)^T H_i C^\perp,$$

the expressions in (13) and (14) are rewritten in the form of  $\mathbf{y}^T \tilde{H}_0 \mathbf{y}$  and  $\mathbf{y}^T \tilde{H}_i \mathbf{y}$ , respectively.

The vector  $\mathbf{y}$  that maximizes the in-band energy of  $p(t)$  subject to the constraints that it has a continuous phase, a (quasi) uniform envelope, and satisfies the zero-ISI condition is obtained as a solution to the following non-linear optimization problem:

$$\begin{aligned} \max_{\mathbf{y}} \quad & \mathbf{y}^T \tilde{H}_0 \mathbf{y} \\ \text{(NLP)} \quad \text{s. t.} \quad & \mathbf{y}^T \tilde{H}_i \mathbf{y} = 0 \quad i = 1, \dots, I \\ & \mathbf{y}^T \mathbf{y} = 1 \end{aligned}$$

A detailed local and global analysis of (NLP) has been presented in [4], and conditions for the global optimality and uniqueness of a stationary point have been derived. It has been shown that all stationary points of (NLP) are eigenvectors of the affine combination  $A(\boldsymbol{\lambda}) = \tilde{H}_0 + \sum_{i=1}^I \lambda_i \tilde{H}_i$ , where  $\boldsymbol{\lambda} = [\lambda_1, \dots, \lambda_I]^T$  is the vector of Lagrange multipliers. Furthermore, the optimal value of (NLP) is related to the largest eigenvalue  $\sigma_1(\boldsymbol{\lambda})$  of  $A(\boldsymbol{\lambda})$  and it is shown that  $\sigma_1(\boldsymbol{\lambda})$  is the appropriate *dual* function for (NLP). The approach taken in [4] is to solve the dual optimization problem, which is an unconstrained minimization of  $\sigma_1(\boldsymbol{\lambda})$ . It is pointed out that unlike general non-linear optimization problems, computation of the dual function in the above case poses no conceptual or computational difficulties. Coupled with the fact that the dual problem has no explicit constraints, it is solved in an efficient manner.

For certain matrices  $\tilde{H}_i$  however, there might exist a duality-gap between (NLP) and its dual [8]. In such cases, solving the dual problem does not yield a solution to the primal, and advanced techniques must be employed that *convexify* the problem [8]. In the optimization procedure described in [4], the duality gap—if it exists—is revealed during the minimization of  $\sigma_1(\boldsymbol{\lambda})$ , else a globally optimal vector  $\mathbf{y}$  is returned. For the design examples presented in the following section, however, a duality gap was not detected.

## V. DESIGN EXAMPLES

In this section, we present several examples of the PSWF based chip waveforms obtained via solving (NLP) by the dual procedure described above. The resulting pulses are denoted as *pswf* pulses in the following. The parameter  $\kappa$  is set to 0.75, which implies that the matched pulse  $g(t)$  is supported on the interval  $[-1.5T_c, 1.5T_c]$ . The performance of the resulting pulses is compared with the half-sine (*msk*), the time-domain raised-cosine (*tdrc*), the zeroth PSWF ( $\psi_0$ ), and pulses reported in [5] (*min*  $M_c$ ); which are all strictly *full-response*, *i.e.* have  $\kappa = 0.5$ . For *pswf* and *min*  $M_c$ , we present results for pulses that have a quasi uniform envelope, and those without. The corresponding pulses are denoted as *QUE* and *NUE* respectively. All pulses have continuous phase except for  $\psi_0$ , which is nonzero at  $T_c/2$ .

The *pswf* matched pulse  $g(t)$  is plotted in Fig. 1, which shows that the essentially full-response property is indeed present. The maximum amplitude of the tail of  $g(t)$  is of the order  $10^{-3}T_c$ . As a result, its contribution to the received SINR, which is given by the second term in (6), is bounded as

$$\frac{1}{T_c^3} \int_{T_c}^{2\kappa T_c} g^2(\tau) d\tau \leq (2\kappa - 1) \max_{\tau \in [T_c, 2\kappa T_c]} g^2(\tau) \leq 10^{-9},$$

and is negligible for all practical purposes.

Fig. 2 shows the minimum bandwidth requirement  $W$  as a function of  $\eta$  in the range  $10^{-2}$ – $10^{-5}$ . A lower bound for the minimum bandwidth among *full-response* pulses is provided by  $\psi_0$ . It is seen that the *pswf* pulses are considerably more bandwidth efficient than both the *msk* and the *tdrc* pulses.

Fig. 3 compares  $M_c \times WT_c$  against  $\eta$  for various pulses. Recall that the product  $M_c \times WT_c$  is indicative of system capacity. We note that the *pswf* pulses achieve the same level of performance as the *min*  $M_c$  pulses which are explicitly designed to minimize  $M_c$ . This is true for both *QUE* and *NUE* pulses. While the *pswf* (*NUE*) pulse achieves almost the same system capacity as  $\psi_0$ , the latter has a discontinuous phase. A comparison with *msk* and *tdrc* pulses for  $\eta = 10^{-5}$  reveals a gain in system capacity by a factor 150% and 500% respectively when the uniform envelope constraint is imposed. The corresponding gains increase to 200% and 700% when the uniform envelope constraint is removed.

The AM-indices of the various pulses are shown in Fig. 4. The *msk* pulse has a constant envelope (or AM-index=0), while the *tdrc* pulse has an AM-index of 17%. Note that while the in-band energy concentration of *pswf* and  $\psi_0$  increases with increasing  $WT_c$  according to Fig. 2, the *min*  $M_c$  pulses were constructed while constraining  $\eta$  to  $10^{-2}$  and  $10^{-3}$  for all values of  $WT_c$ . The *NUE* pulses in the top sub-plot were obtained by solving (NLP) without the uniform envelope constraint (11). All pulses in this category show an increasing AM-index with increasing  $WT_c$ . We see that the *pswf* pulse shows the lowest envelope variation followed by  $\psi_0$ , while the *min*  $M_c$  pulses have a substantially larger envelope variation. Among the *QUE* pulses, at  $WT_c \approx 2.2$ , all three pulses have nearly the same AM-index. However, while the *pswf* pulse

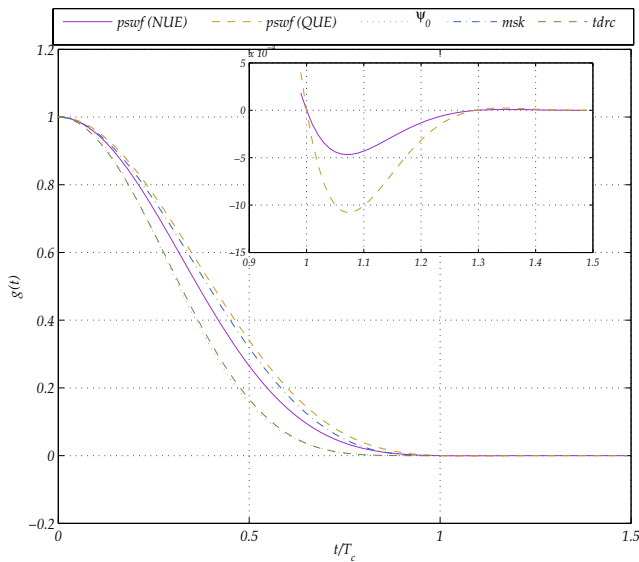


Fig. 1. Matched pulses

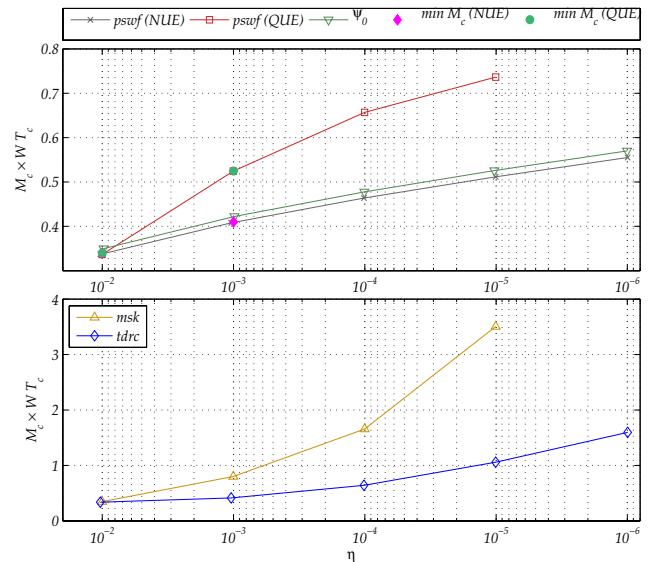


Fig. 3. Mean squared correlation

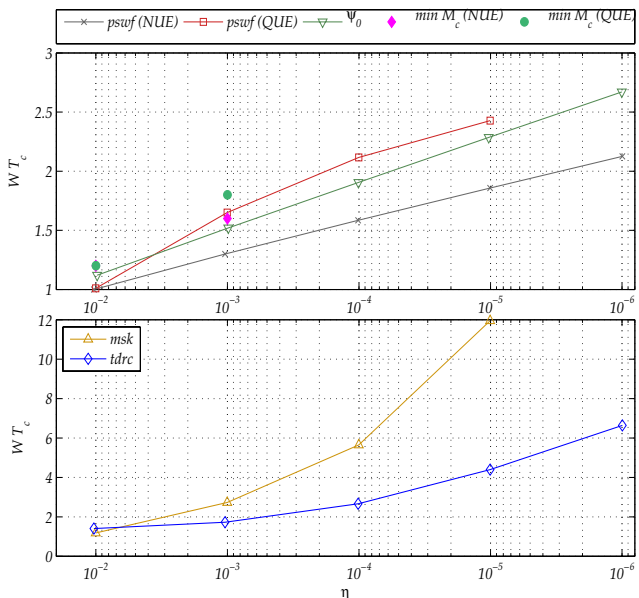


Fig. 2. Bandwidth efficiency

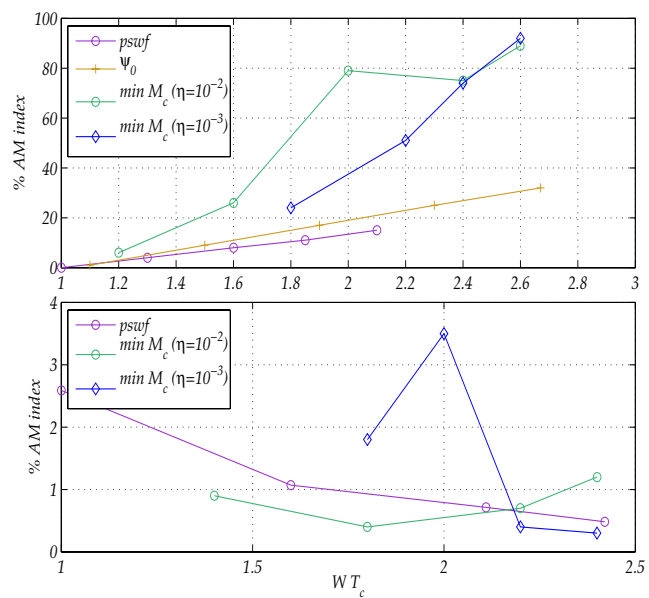


Fig. 4. AM index for NUE (top) and QUE (bottom) pulses

has an  $\eta = 10^{-4}$ , the  $\min M_c$  pulses have substantially more out of band energy leakage at  $\eta = 10^{-2}$  and  $\eta = 10^{-3}$ .

### VI. CONCLUSIONS

An optimization procedure is presented for the design of DS-CDMA chip-waveforms that have the maximum in-band energy concentration of the power spectrum while at the same time have smooth phase transitions and a nearly constant envelope of the transmitted signal. The resulting waveforms show considerable gains in system capacity compared to conventional modulation schemes including MSK and time-domain raised-cosine pulses.

### REFERENCES

[1] R. Anjaria and R. Wyrwas, "The effect of chip waveform on CDMA systems in multipath fading noisy channels," in *Proc. IEEE 42nd VTS Conf.*, Denver, CO, May 1992, pp. 672–675.

[2] P. I. Dalls and F. N. Pavlidou, "Innovative chip waveforms in microcellular DS/CDMA packet mobile radio," *IEEE Trans. Commun.*, vol. 44, no. 11, pp. 1413–1416, Nov. 1996.

[3] Y. C. Yoon, "Quadrphase DS-CDMA with pulse shaping and the accuracy of the gaussian approximation for matched filter receiver performance analysis," *IEEE Trans. Wireless Commun.*, vol. 1, no. 4, pp. 761–768, Oct. 2002.

[4] R. Sood and H. Xiao, "Root nyquist pulses with and energy criterion," in *Proc. IEEE ICC 07*, Glasgow, Jun. 2007, pp. 2711 – 2716.

[5] M. A. Landolsi and W. E. Stark, "DS-CDMA chip waveform design for minimum interference under bandwidth, phase, and envelope constraints," *IEEE Trans. Commun.*, vol. 47, no. 11, pp. 1737–1746, Nov. 1999.

[6] M. B. Pursley, F. D. Garber, and J. S. Lehnert, "Analysis of quadrphase spread-spectrum communications," in *Proc. IEEE ICC*, vol. 1, Jun. 1980, pp. 15.3.1–15.3.6.

[7] D. Slepian and H. O. Pollak, "Prolate spheroidal wave functions, Fourier analysis, and uncertainty - I," *Bell Syst. Tech. J.*, vol. 40, no. 1, pp. 43–63, Jan. 1961.

[8] D. G. Luenberger, *Linear and Non Linear Programming*, 2nd ed. Reading, Mass: Addison Wesley, 1984.